
A UNIFIED THEORY AND STATISTICAL LEARNING APPROACH FOR TRAFFIC CONFLICT DETECTION

Yiru Jiao^{1,3,*}, Simeon C. Calvert^{1,3}, Sander van Cranenburgh^{2,3}, Hans van Lint¹

¹ Department of Transport & Planning,

² Department of Engineering Systems and Services,

³ CityAI lab,

Delft University of Technology, Delft, the Netherlands

ABSTRACT

This study proposes a unified theory and statistical learning approach for traffic conflict detection, addressing the long-existing call for a consistent and comprehensive methodology to evaluate the collision risk emerging in road user interactions. The proposed theory assumes context-dependent probabilistic collision risk and frames conflict detection as assessing this risk by statistical learning of extreme events in daily interactions. Experiments using real-world trajectory data are conducted in this study, where a unified metric of conflict is trained with lane-changing interactions on German highways and applied to near-crash events from the 100-Car Naturalistic Driving Study in the U.S. Results of the experiments demonstrate that the trained metric provides effective collision warnings, generalises across distinct datasets and traffic environments, covers a broad range of conflicts, and delivers a long-tailed distribution of conflict intensity. Reflecting on these results, the unified theory ensures consistent evaluation by a generic formulation that encompasses varying assumptions of traffic conflicts; the statistical learning approach then enables a comprehensive consideration of influencing factors such as motion states of road users, environment conditions, and participant characteristics. Therefore, the theory and learning approach jointly provide an explainable and adaptable methodology for conflict detection among different road users and across various interaction scenarios. This promises to reduce accidents and improve overall traffic safety, by enhanced safety assessment of traffic infrastructures, more effective collision warning systems for autonomous driving, and a deeper understanding of road user behaviour in different traffic conditions.

Keywords Traffic safety · autonomous driving safety · conflict detection · collision risk · Surrogate Measures of Safety

*Correspondence: y.jiao-1@tudelft.nl

1 Introduction

Collision avoidance and accident prevention are key elements in efforts to improve traffic safety (Vahidi and Eskandarian 2003; Zheng, Sayed, et al. 2021). Motivated by proactive prevention of accidents and not waiting for collisions to happen, Surrogate Measures of Safety were proposed as surrogates of real collisions for safety evaluation and improvement. Over the past decades, traffic conflicts have become one of the most comprehensive and prominent surrogates (Zheng, Ismail, et al. 2014b; Tarko 2018). A traffic conflict is defined as “an observable situation in which two or more road users approach each other in space and time to such an extent that there is a risk of collision if their movements remain unchanged” (P. Cooper 1977). Under this definition, every conflict is a potential collision; and every collision is a conflict until the moment when it becomes unavoidable. Despite the relative rareness when compared with safe daily interactions, successfully resolved conflicts that do not end in collisions offer opportunities to explore the emergence and resolution of collision risk (Tarko 2018). This has been widely recognised in the traffic safety community, and is being adopted in emerging technologies such as driving assistance and autonomous driving.

Conflicts cannot always be directly measured due to the unclear boundary between safe and unsafe interactions, thus conflict detection often relies on surrogate metrics. These metrics are called “conflict/safety indicators” in the field of traffic safety (Vogel 2003) or “criticality metrics” in the field of autonomous driving (Junietz et al. 2018). This difference in terminology implies different focuses on the scale of their respective research objective. Traffic safety studies concentrate more on reasoning about the contributing factors of collisions and reducing accidents in general; while autonomous driving studies aim to ensure safe interactions between automated vehicles and other road users (Razi et al. 2022). As a result, conflict indicators are predominantly used for identifying contributing factors of collisions (Saunier, Mourji, et al. 2011; Wu and Jovanis 2012) and evaluating the safety of transportation infrastructure, a traffic signal system, or a specific type of interaction (Saunier, Sayed, et al. 2007; Laureshyn et al. 2010; de Ceunynck 2017). In contrast, criticality metrics are more used for predicting trajectories of other road users (X. Wang et al. 2022), developing driving strategies (L. C. Das and Won 2021), and assessing individual collision risk (Broadhurst et al. 2005; Kim and Kum 2018; Zhou and Zhong 2020). In this paper, we use surrogate metrics of conflicts to uniformly refer to both conflict/safety indicators and criticality metrics.

A variety of surrogate metrics of conflicts have been developed for different types of interactions. For instance, Deceleration Rate to Avoid Collision (DRAC, D. F. Cooper and Ferguson 1976) and its variants are primarily targeted at rear-end conflicts. Time-To-Collision (TTC, Hayward 1972; Hydén 1987) along with its variants can cover both rear-end and side-swipe conflicts. Time advantage (Laureshyn et al. 2010), also known as predicted Post-Encroachment-Time (PET), is specifically tailored for path-crossing conflicts. In addition, composite indices are designed by integrating multiple metrics to deal with more complicated conflicts such as those during lane changes (Uno et al. 2002; Li et al. 2017). Many summaries (to name a few, Arun, Haque, Bhaskar, et al. 2021; Arun, Haque, Washington, et al. 2021; Lu et al. 2021; C. Wang et al. 2021; Westhofen et al. 2022) are available for an overview of these metrics, and new metrics are being proposed for interactions in a two-dimensional plane (Ward et al. 2015; Venthuruthiyil and Chunchu 2022) and in traffic oscillations (Kuang et al. 2015; Y. Wang et al. 2024).

The diversity of these metrics entails inconsistency as collision risk is heterogeneous in different traffic conditions, between different vehicles, and is subject to changes in road user behaviour (Mannering et al. 2016; Zheng, Sayed, et al. 2021). Some experiments show that the perception of critical TTC can vary among drivers (Kusano et al. 2015) and in different traffic environments (Tageldin and Sayed 2019; Arun, Haque, Washington, et al. 2021; Chauhan et al. 2022). For example, a TTC of 3 seconds could be dangerous for vehicles rushing on highways, but not necessarily for vehicles making a cooperative lane-change, nor for vehicles decelerating to approach an urban intersection. Similarly, a 2-second PET could be accident-prone for cars crossing their paths at an intersection, but is not uncommon for cyclists (Beitel et al. 2018). In addition, with the increasing prevalence of driving assistance systems and electric vehicles, behavioural changes in interaction may gradually influence people’s perception of collision risk (T. Das et al. 2022; Wessels et al. 2022).

Increasing efforts are devoted to addressing these inconsistencies. However, two major challenges remain. The first is a one-for-all metric integrating various surrogate metrics of conflicts that make different assumptions and consider different aspects of collision risk. To this end, there is a growing trend towards combining multiple metrics (e.g., Kuang et al. 2015; Nadimi, Amiri, et al. 2021; Mazaheri et al. 2023), particularly by applying deep learning (Formosa et al. 2020; Abdel-Aty et al. 2023). Such a combination builds understanding from existing metrics, but meanwhile is constrained by their assumptions. The second challenge lies in determining a robust threshold, for a metric or a combination of multiple metrics, to distinguish unsafe conflicts from safe interactions. If there is ground truth, the threshold should optimise the accuracy of conflict identification for, e.g., issuing crash warnings (L. C. Das and Won 2021). When no label is available, the threshold selection often follows heuristic rules (Panou 2018; S. Das and Maurya 2020; Nadimi, NaserAlavi, et al. 2022), or is based on extreme value theory to satisfy certain hypotheses (Farah and Azevedo 2017; Borsos et al. 2020).

To provide a methodology for consistent and comprehensive conflict detection, the aim of this study is twofold. First, we present a unified theory of traffic conflicts, deductively from a general probabilistic description of collision risk. Second, we propose a statistical learning approach that applies the theory to practical conflict detection. Our theory considers a traffic conflict as an extreme event of normal interactions, and quantifies its context-dependent and proximity-characterised collision risk. Then the learning approach breaks down conflict detection into three tasks of interaction context representation, proximity distribution inference, and extreme event assessment. Theoretically, any existing surrogate metric of conflicts is a special case under the theory, and our statistical learning approach can be generally applied to varying traffic conditions and all categories of road users.

The rest of this paper is organised as follows. Section 2 first introduces and explains the unified theory of traffic conflicts. Then Section 3 provides a statistical learning approach to apply the unified theory to conflict detection, including probability estimation and conflict intensity evaluation. In Section 4, demonstration experiments are designed, performed, and analysed to show the characteristics of applying the theory and learning approach. Finally, Section 5 concludes this paper and envisions future research.

2 A unified theory of traffic conflicts

This section introduces our unified theory of traffic conflicts. In the theory, we treat conflict detection as quantifying the risk of a potential collision c between two or more road users, based on their proximity s and other contextual observables X , i.e., $p(c|s, X)$. This risk quantification uses Bayesian probability to consider the interaction situation of an event, the typical proximity behaviour of road users in the interaction context, and the probability variation with conflict intensity. These considerations are summarised in Equation (1) for a preliminary overview, where the symbols are defined in Table 1.

$$p(c|s, X) = \iint p(c|s, \phi)p(\phi|\theta)p(\theta|X)d\phi d\theta, \text{ where } p(c|s, \phi) := C(n; s, \phi) \quad (1)$$

Table 1. Symbols and their definitions in the unified theory of conflict detection.

Symbol	Definition
c	A potential collision, i.e., conflict
s	Proximity, the spatial-temporal closeness between road users
X	Observables that can be measured to describe interaction situations
θ	Representation for the interaction context involving key information selected from X
ϕ	Parameters used to characterise the proximity distribution of road users in a given θ
n	Conflict intensity, a conflict at intensity n occurs once per n times in the same interactions
C	Probability of a conflict with intensity n at proximity s in the context characterised by ϕ

Subsequent subsections present explanations and derivations to establish the theory, where we integrate probabilistic methods, behavioural insights, and statistical modelling to estimate and evaluate the collision risk in varying interaction contexts. We begin with defining the probabilistic collision risk that depends on proximity and other situational variables. Then we assume a conflict hierarchy of risk perceptions and reactions in an interaction situation, and describe the conflict hierarchy quantitatively by measuring how road user behaviour varies with proximity. Lastly, we consider conflicts as extreme events within a spectrum of interactions, and use extreme value theory to relate conflict probability with conflict intensity.

2.1 Context-dependent collision risk

In this subsection, we first present a general probabilistic description of conflict detection which depends on the context of interaction. A major branch of surrogate metrics of conflicts is based on proximity. Proximity means physically less space and time for reactions to prevent a potential collision; and due to the physical constraints, people perceive increased risk when the distance to an approaching object is closer (Schiff and Detwiler 1979; Teigen 2005). Therefore, a proximity-based conflict metric can cover both the objective aspect of collision risk, but also people’s subjective perception of the collision risk.

Proximity-based conflict detection can be generally formulated as shown in Equation (2), which estimates the probability of a potential collision c based on proximity s ($s \geq 0$) and other observables X of the interaction situation. For an interaction involving two or more road users, s is a measure of the spatial-temporal closeness between the road users;

and X can include, but is not limited to, motion states of the road users, traffic states, road layouts, and weather. The probability is between 0 and 1 for consistent comparison.

$$p(c|s, X) \quad (2)$$

Not all of the information in X is used, nor might it all be useful. Every existing surrogate metric of conflicts selects some key information, i.e., variables, and makes assumptions based on the selected information. For example, TTC uses the relative velocity between two approaching road users and assumes no movement change (zero acceleration) at the moment of conflict; DRAC also uses the relative speed but assumes an immediate brake. Here we use $\theta = \{\theta_1, \theta_2, \dots, \theta_k\}$ to denote k variables selected from X , and θ are assumed to adequately represent the interaction context compressed out of the situation X . Considering all possible selections of θ , Equation (2) equals Equation (3) according to Bayes' theorem.

$$p(c|s, X) = \int p(c|s, \theta)p(\theta|X)d\theta \quad (3)$$

If the selection of key information is deterministic as $\theta = \mathbb{R}(X)$, where \mathbb{R} refers to representation learning of the interaction context, $p(\theta|X)$ in Equation (3) becomes a Dirac delta function of $\delta(\theta - \mathbb{R}(X))$. A Dirac delta function $\delta(x)$ has a value of 1 when $x = 0$ and 0 for any other values of x . Therefore, Equation (3) can be approximated to Equation (4)

$$p(c|s, X) = p(c|s, \theta) = p(c|s, \mathbb{R}(X)), \text{ if } p(\theta|X) = \delta(\theta - \mathbb{R}(X)) \quad (4)$$

To better explain how a surrogate metric of conflicts fits into our formulation, we provide two examples. The first is Post-Encroachment Time (PET), where s is the time interval between one vehicle leaving a conflict area and another vehicle arriving in the same conflict area. The θ for PET is the existence of a conflict area. As shown in Figure 1a, $p(c|s, \theta)$ can be a step function with probability 1 when PET exceeds a threshold PET^* and 0 otherwise; or a continuous function based on a cumulative Gaussian probability that increases gradually from 0 to 1 and is 0.5 at the threshold PET^* . Then another example uses $TTC = s/\Delta v$ as shown in Figure 1b. For two vehicles approaching each other, s is the net distance between them; while Δv is their relative speed, and serves as a univariate context θ . The probability $p(c|s, \theta)$ varies at different relative speeds. If there is a critical threshold TTC^* that differentiates safe and unsafe interactions, the threshold of proximity then follows $s^* = TTC^* \Delta v$.

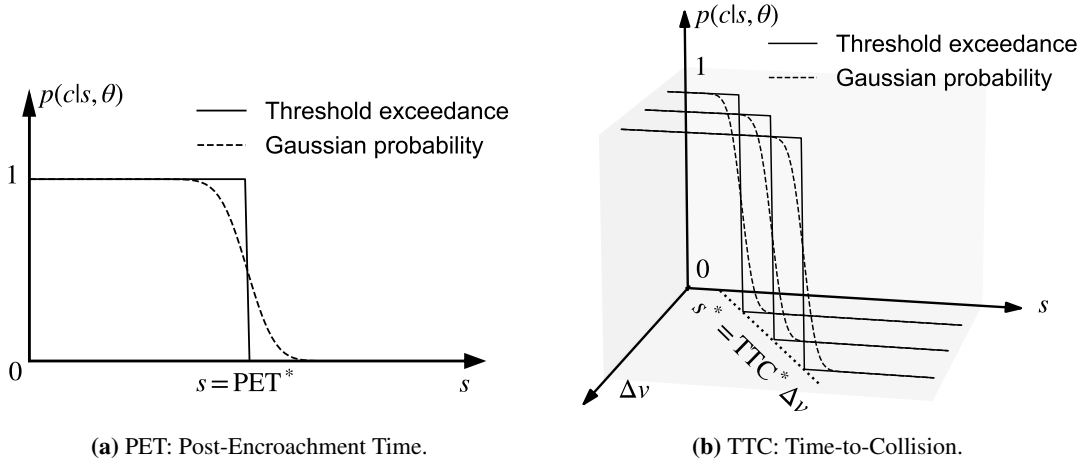


Figure 1. Illustration examples of context-dependent proximity-based conflict probability.

2.2 Proximity-characterised conflict hierarchy

Proximity patterns in an interaction context reflect the aggregated behaviour of road users in this context, which is shaped by people's perception of collision risk. Within the same context of interaction situations, a shorter spatial or temporal gap between road users consistently implies more risk of collision. This increase in collision risk with decreasing proximity motivates road users to maintain an acceptable distance from the others at varying levels (Camara and Fox 2020). Therefore, the proximity behaviour of road users embodies a conflict hierarchy perceived by the road users. On the one hand, proximity pushes or prevents the road users from approaching each other; on the other hand, the road users adjust their behaviours to maintain comfortable proximity.

We characterise the proximity behaviour of road users with a conditional probability distribution. Seeing proximity as a random variable S , in a certain interaction context θ , the conditional probability distribution of S given a context θ is $p(s|\theta)$. We use $f_S(s|\theta; \phi)$ to describe the density function of $p(s|\theta)$, where ϕ is a set of parameters. To incorporate context-dependent proximity behaviour into conflict detection, we consider all possible sets of ϕ in a context θ , thus integrate $p(\phi|\theta)$ in Equation (5) according to Bayes' theorem.

$$p(c|s, \theta) = \int p(c|s, \phi)p(\phi|\theta)d\phi \quad (5)$$

As we parameterise the conditional probability $p(s|\theta)$ with $f_S(s|\theta; \phi)$, inferring $p(s|\theta)$ is to obtain ϕ , and we denote this inference as $\phi = \mathbb{I}(\theta)$. When the inference is deterministic, $p(\phi|\theta)$ in Equation (5) becomes a Dirac delta function $\delta(\phi - \mathbb{I}(\theta))$. In the same way as explained when deriving Equation (4), we can derive Equation (6).

$$p(c|s, \theta) = p(c|s, \phi) = p(c|s, \mathbb{I}(\theta)), \text{ if } p(\phi|\theta) = \delta(\phi - \mathbb{I}(\theta)) \quad (6)$$

Numerous empirical studies have observed the transition from comfort to discomfort when a road user is approached by other vehicles (Taieb-Maimon and Shinar 2001; Lewis-Evans et al. 2010; Siebert, Oehl, and Pfister 2014; Siebert, Oehl, Bersch, et al. 2017). Therefore, we can generally assume that $p(c|s, \phi)$ monotonically increases while s is decreasing. In a conflict hierarchy characterised by ϕ , the closer the proximity between approaching road users, the less safe they are and the higher the probability of a potential collision. This monotonicity of $p(c|s, \phi)$ implies that Equation (7) holds for any ϕ .

$$\begin{cases} \lim_{s \rightarrow \infty} p(c|s, \phi) = 0 \\ \lim_{s \rightarrow 0} p(c|s, \phi) = 1 \end{cases} \quad (7)$$

Figure 2 helps explain the proximity-characterised conflict hierarchy. On the left of Figure 2, we present an adapted pyramid of conflict hierarchy (Hydén 1987), which conceptually relates conflict intensity and frequency, and reflects road user behaviour in balancing safety and efficiency (Laureshyn et al. 2010). When the approaching between road users entails a potential collision, the closer they are, the higher the conflict intensity and the lower the frequency of such conflicts. When the proximity is too small for safe interaction, a conflict emerges entailing a potential collision. Furthermore, an accident will happen if there is no (successful) evasion or the proximity is too small to prevent a collision. As illustrated in the right of Figure 2, $f_S(s|\theta; \phi)$ is designed to capture the shape of the pyramid hierarchy in different interaction contexts. Therefore, the estimated probability $p(c|s, \phi = \mathbb{I}(\theta))$ may vary for the same proximity in different contexts, and evolve as the interaction context changes over time.

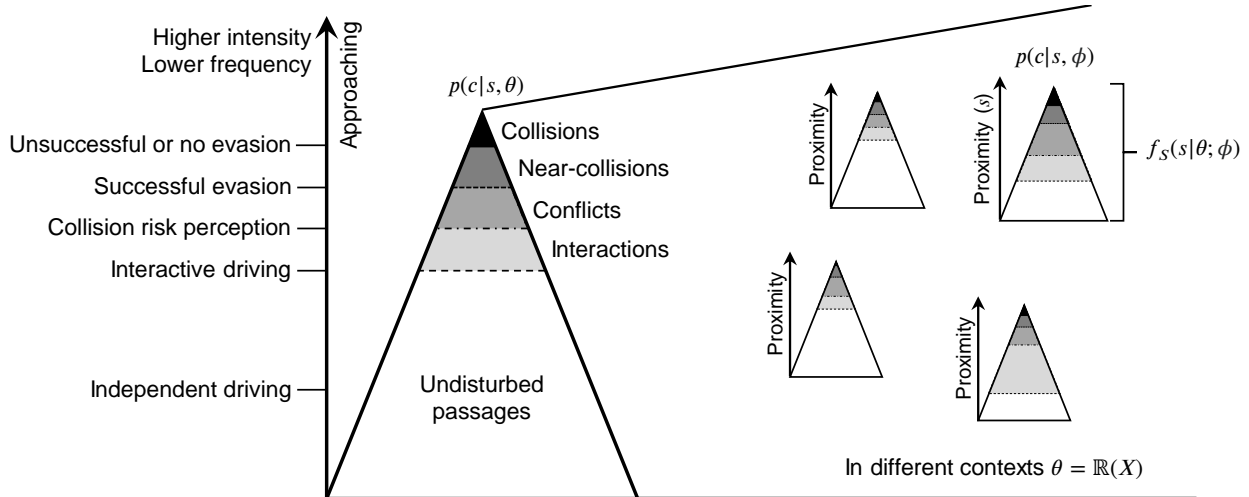


Figure 2. Proximity-characterised conflict hierarchy varies in different interaction contexts.

2.3 Extreme value theory-based interaction spectrum

Traffic interactions exist on a spectrum varying in conflict intensity and potential consequences. Within this spectrum, we assume that conflicts are extreme events at different levels of collision risk. Then we can establish the relationship between conflict intensity and conflict probability utilising extreme value theory. Extreme value theory has been

traditionally used to treat crashes as the extreme events of conflicts (Songchitruksa and Tarko 2006; Zheng, Ismail, et al. 2014a; Farah and Azevedo 2017; Tarko 2021). Here we zoom out the view and see conflicts as the extreme events of general interactions, at varying levels of intensity.

Our derivation uses a similar logic to lifetime survival analysis, which is a branch of statistics to model the expected duration of time until one event, such as deaths or failures of medical treatment, occurs (Reiss and Thomas 1997). The essential idea of lifetime survival analysis is to estimate the probability of events from the records of human lives or running systems, where the frequency of these events reduces when living time increases. Therefore, the survival function is $S(t) = \Pr(T > t)$, representing the cumulative probability that the duration of survival T is longer than some specified time t . The longer the t , the closer to death or failure.

When estimating the probability of conflicts, failures are collisions, and our evaluation is based on the records of daily interactions. In lifetime survival analysis, the measure is survival duration and *longer* duration is closer to deaths; whereas in analysing conflicts, the measure is proximity and *shorter* proximity is closer to conflicts. The frequency of conflicts thus increases when proximity reduces. We define a “conflict” function $F(s) = \Pr(S < s)$, which represents the cumulative probability that the interaction proximity S is less than a certain s . Recall that in Section 2.2 we use the function $f_S(s|\theta; \phi)$ to describe the proximity distribution of S in an interaction context θ . Given that $\phi = \mathbb{I}(\theta)$ and $\theta = \mathbb{I}^{-1}(\phi)$, this function can be rewritten as $f_S(s; \phi)$ for convenience. Then Equation (8) shows the conflict function in an interaction context θ where the conflict hierarchy is characterised by ϕ .

$$\begin{aligned} F(s; \phi) &= \Pr(S < s; \phi) \\ &= \int_0^s f_S(x; \phi) dx \end{aligned} \quad (8)$$

The shorter the s , the more likely a conflict is to occur, but the likelihood varies with conflict intensity. Aligned with the conflict hierarchy in Figure 2, we define conflict intensity as the inverse of conflict frequency, i.e., a conflict at intensity n occurs once per n times in the same interaction situations. Specifically, assuming an interaction where the proximity between road users is s ; if s is always smaller than the observed proximities for n times interactions in the same situation, this interaction is a conflict with a frequency of $1/n$, and we consider it an extreme event at intensity n . Accordingly, we can use $(\Pr(S \geq s; \phi))^n$ to calculate the cumulative probability that a proximity s is the minima in n times of observations in the same interaction context. Therefore, for an interaction at proximity s and in the context θ that is characterised by ϕ , its probability of conflict is not a value, but a function concerning conflict intensity n . We denote this function by C as shown in Equation (9).

$$\begin{aligned} p(c|s, \phi) &:= C(n; s, \phi) \\ &= \left(\int_s^\infty f_S(x; \phi) dx \right)^n \end{aligned} \quad (9)$$

Equation (9) fulfils the requirements in Equations (7) and monotonically increases while s decreases. This denotation thus corresponds to the practical understanding of a conflict: the smaller the proximity and the lower the conflict intensity, the greater the conflict probability. When n is very large and approaches infinity, which means the most intense and least frequent interaction, i.e. collision, Equation (9) converges to either Gumbel, Frechet, or Weibull distribution. Here we do not particularly consider this convergence at an infinite n , as our evaluation focuses not only on collisions, but on conflicts at varying levels of intensity.

3 A statistical learning approach for conflict detection

The previous section introduces and explains the theoretical foundation of conflict detection. Now we continue by giving a statistical learning approach to apply this theory. Based on the derivation in Section 2, we can decompose conflict detection into three tasks as shown in Figure 3. The first task $\theta = \mathbb{R}(X)$ maps situational observables X to a compressed information space as θ , which represents interaction context. In a certain interaction context θ , the second task $\phi = \mathbb{I}(\theta)$ infers the conditional probability distribution of typical proximity behaviour of road users. Then the third task uses extreme value theory to determine the relationship between conflict intensity and probability. When $\theta = \mathbb{R}(X)$ and $\phi = \mathbb{I}(\theta)$ are deterministic, we can rewrite Equation (1) into Equation (10).

$$\begin{aligned} p(c|s, X) &= \iint p(c|s, \phi) p(\phi|\theta) p(\theta|X) d\phi d\theta = p(c|s, \phi) := C(n; s, \phi), \\ &\text{if } p(\theta|X) = \delta(\theta - \mathbb{R}(X)) \text{ and } p(\phi|\theta) = \delta(\phi - \mathbb{I}(\theta)) \end{aligned} \quad (10)$$

These three tasks can be integrated within a pipeline for end-to-end learning, and can also be performed separately. In the following subsections, we will explain the tasks further and present a preliminary approach for application. We

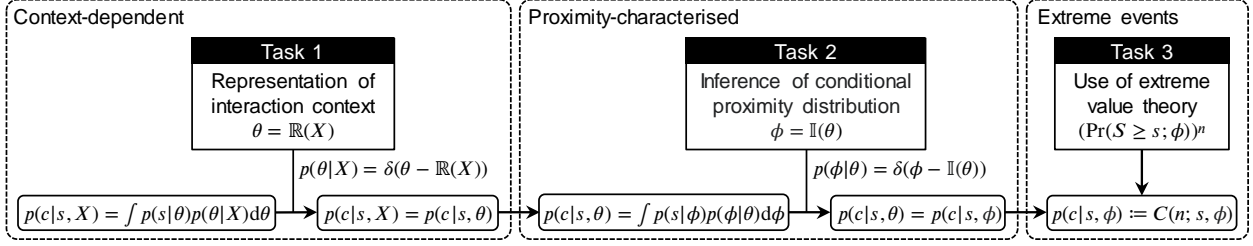


Figure 3. Task decomposition of conflict detection.

emphasise here that there are many useful learning methods, and the ones we use in this study are not necessarily the best. Future investigation on optimising suitable statistical learning techniques is required.

3.1 Representation of interaction context

The first task $\theta = \mathbb{R}(X)$ is to create an informative representation for interaction contexts by selecting and transforming relevant observables of interaction situations. Traditionally, key variables such as absolute speed, relative speed, and deceleration rate have been widely validated and used in existing measures. However, there may be more factors at play than those hypothesised in the existing measures. As mentioned in Section 2.1, X may cover various aspects such as vehicle motion states, environment factors, and participant characteristics. Incorporating different factors can be particularly helpful for a comprehensive assessment of collision risk and for user-customised collision warnings.

We have some notes on learning representations from variables relevant to motion states. Firstly, the output in the next task of inference is about the proximity between interacting road users. To avoid label leakage, we recommend not including a complete series of position or speed vectors for all involved road users. Secondly, we suggest transforming the variables into local coordinate systems. This transformation can be centred on every road user involved in an interaction situation, as the same situation may be perceived differently by different road users. Such view transformation can ensure the consistency and enhance the comparability of interaction context representations. Once transformed, an interaction context can be represented as instantaneous frames or over a continuous period.

If the observables of an interaction situation are numerous or use time-series and/or image formats, data-driven representation learning can be effectively employed. Such techniques can compress selected observables into a lower-dimensional space, where different interaction contexts are adequately encapsulated. One approach can be auto-encoders, of which the learning objective is to minimise the reconstruction error between compressed representation and original information. Another approach is contrastive learning, which aims to minimise the difference between the representations of similar situations while maximising the difference between dissimilar situations. Representation learning is an active and evolving field in machine learning, where many other methods are worth investigating. It is important to note that purely data-driven methods may not always capture the nuances of complex interaction situations. Therefore, integrating domain knowledge in traffic safety is necessary and can improve the robustness and reliability of context representation.

3.2 Inference of conflict hierarchy

The second task $\phi = \mathbb{I}(\theta)$ needs to learn the conditional probability distribution of proximity in a certain interaction context, i.e., $p(s|\theta)$. Our previous study (Jiao et al. 2023) used conditional sampling to infer this probability. Such sampling requires a large amount of data to ensure enough samples for each condition range, while the condition ranges are finite samples of an infinite space. In this study, we use Gaussian Process Regression (GPR) to avoid discretising the condition space, and the rest of this subsection will explain more details. Note that there are other useful methods to learn the conditional probability, but we choose GPR in order to obtain the equation of $p(s|\theta)$ and thus its analytical cumulative probability.

Many studies have found that the lognormal distribution best fits the distribution of spatial and temporal gaps between road users (Meng and Qu 2012; Pawar and Patil 2016; Anwari et al. 2023). Therefore, we assume that the proximity s in a certain interaction context θ follows a lognormal distribution. Recall that in Section 2.2 we use $f_S(s|\theta; \phi)$ to describe $p(s|\theta)$, and now we have $\phi = \{\mu, \sigma\}$ where μ and σ parameterise a lognormal distribution as in Equation (11). This implies that the logarithm of proximity, $\ln(s)$, follows a Gaussian distribution that is parameterised by the same μ

and σ .

$$f_S(s|\theta; \mu, \sigma) = \frac{1}{s\sigma\sqrt{2\pi}} \exp\left(-\frac{(\ln(s) - \mu)^2}{2\sigma^2}\right) \quad (11)$$

The Gaussian distribution of $\ln(s)$ can be utilised to learn $p(s|\theta)$ with GPR. First, we consider a mapping $g : \theta \rightarrow \ln(s)$ between proximity s and the interaction context θ that s is in. Assuming a normally distributed noise in this mapping, we denote that $\ln(s) = g(\theta) + \epsilon$, where $\epsilon \sim \mathcal{N}(0, \sigma_\epsilon^2)$. Second, given that $\ln(s)$ is derived to be normally distributed, the distribution of function $g(\theta)$ is Gaussian. Then we can consider that $g(\theta)$ is drawn from a Gaussian Process, as shown in Equation (12). This suggests that a $g(\theta)$ is one sample from the multivariate Gaussian distribution of all possible relationships.

$$g(\theta) \sim \mathcal{GP}(m(\theta), K(\theta, \theta')), \quad (12)$$

where $\mu = m(\theta)$ and $\sigma = K(\theta, \theta')$ are the mean function and covariance function that specify a Gaussian Process. For two similar interaction contexts θ and θ' , $g(\theta)$ is expected to be close to $g(\theta')$.

With GPR, the mean and covariance functions are learned from data. Considering that we may include many variables in the representation of interaction context and thus a fairly large amount of data is needed to serve training, here we use the Scalable Variational Gaussian Process (SVGP) model with the python library GPyTorch (Gardner et al. 2018). As the cost to increase scalability, SVGP does not ensure an exact solution and may underestimate variance. To train this model effectively, we maximise a predictive log-likelihood in Equation (13), which is proposed in (Jankowiak et al. 2020) and we adapt it here. In addition to the symbols that we have consistently used, N is the number of samples; u denotes inducing variables that are introduced to perform sparse training and reduce computational load; $q(u)$ is the variational distribution of u ; $p(u)$ is the prior distribution of u ; $D_{\text{KL}}[q(u)||p(u)]$ computes the Kullback–Leibler divergence of $q(u)$ and $p(u)$; and β controls the regularisation effect of KL divergence.

$$\begin{aligned} L &= \mathbb{E}_{p_{\text{data}}(\ln(s), \theta)} [\ln(p(\ln(s)|\theta))] - \beta D_{\text{KL}}[q(u)||p(u)] \\ &\approx \sum_{i=1}^N \ln \left\{ \mathbb{E}_{q(u)} \left[\int p(\ln(s_i)|g_i) p(g_i|u, \theta_i) dg_i \right] \right\} - \beta D_{\text{KL}}[q(u)||p(u)] \end{aligned} \quad (13)$$

Theoretically, learning the mean and covariance functions can approximate any form of mapping between interaction context θ and proximity s . As explained in Sections 2.1 and 2.2, a surrogate metric for traffic conflicts essentially assumes such a mapping, based on which a threshold is then determined to distinguish safe interactions and conflicts. Therefore, in theory, any metric based on spatial-temporal proximity is a particular case under our unified theory, and our statistical learning approach can specify the mapping in data. This suggests that, given the same interaction context, a data-driven metric using the theory and learning approach proposed in this study should be no less conflict-indicative than an assumed metric.

3.3 Conflict probability estimation and intensity evaluation

In the third task, we use extreme value theory to estimate conflict probability and evaluate conflict intensity. This task plays a similar role to the selection of thresholds when using traditional metrics of conflicts. After the previous two tasks, for every interaction situation represented with θ , we can learn parameters $\phi = \{\mu, \sigma\}$ that characterise the conflict hierarchy in different interaction contexts. Based on the derivation in Section 2.3, then we can write conflict function $F(s; \phi)$ and obtain $C(n; s, \phi)$ that relates conflict intensity n and conflict probability.

Given that we infer $f_S(s|\theta; \phi)$ as the probability density function of the lognormal distribution, the conflict function $F(s; \phi)$ in Equation (8) can be further derived as Equation (14). Here $\text{erf}(z) = 2 \int_0^z e^{-x^2} dx / \sqrt{\pi}$ and is the Gaussian error function. Then conflict probability function is as shown in Equation (15).

$$\begin{aligned} F(s; \mu, \sigma) &= \int_0^s \frac{1}{x\sigma\sqrt{2\pi}} \exp\left(-\frac{(\ln(x) - \mu)^2}{2\sigma^2}\right) dx \\ &= \frac{1}{2} + \frac{1}{2} \text{erf}\left(\frac{\ln(s) - \mu}{\sigma\sqrt{2}}\right) \end{aligned} \quad (14)$$

$$\begin{aligned} C(n; s, \mu, \sigma) &= (1 - F(s; \mu, \sigma))^n \\ &= \left(\frac{1}{2} - \frac{1}{2} \text{erf}\left(\frac{\ln(s) - \mu}{\sigma\sqrt{2}}\right)\right)^n \end{aligned} \quad (15)$$

There are two general purposes for conflict detection. The first is conflict probability estimation. For an interaction situation, given current proximity s and parameters ϕ that characterise the conflict hierarchy in the interaction context, we can use Equation (16a) to estimate the probability of a potential collision at different levels of conflict intensity n . The second purpose is safety/conflict evaluation. Assuming that the probability of a potential collision is larger than the probability of no collision, i.e., conflict probability is larger than 0.5, we can use Equation (16b) to evaluate the maximum possible conflict intensity.

$$p = C(n; s, \mu, \sigma) = \left(\frac{1}{2} - \frac{1}{2} \operatorname{erf} \left(\frac{\ln(s) - \mu}{\sigma\sqrt{2}} \right) \right)^n, \quad n \geq 1 \quad (16a)$$

$$n = C^{-1}(p; s, \mu, \sigma) = \frac{\ln p}{\ln \left(\frac{1}{2} - \frac{1}{2} \operatorname{erf} \left(\frac{\ln(s) - \mu}{\sigma\sqrt{2}} \right) \right)}, \quad 0.5 < p < 1 \quad (16b)$$

Equations (16a) and (16b) are useful in different practices. Conflict probability estimation can be used to issue collision warnings, which alert human drivers or driving assistance systems to prevent potential collisions. Conflict intensity evaluation can be used to identify varying levels of conflict cases in daily traffic. This helps to assess the impact of an infrastructure or traffic policies on traffic safety, and then make according improvements.

4 Demonstration

This section applies the proposed unified theory and statistical learning approach on real-world trajectory data, to demonstrate the characteristics of this new conflict detection methodology. Table 2 presents an overview of our experiment design. In Section 4.1, we introduce the datasets we use and experiment details. Then respectively in Sections 4.2 and 4.3, we show the experiment results in conflict probability estimation and conflict intensity evaluation. For convenience, we use *methodology* to collectively refer to the theory and learning approach proposed in this study; and use the term *unified metric* and its abbreviation *Unified* to refer to the surrogate metric trained with our methodology. It is also important to emphasise that these experiments are designed primarily for demonstration. Further exploration is expected in future research.

Table 2. An overview of experiment design for methodology demonstration.

Purpose	Training data	Application data	Characteristics: this methodology
Conflict probability estimation $p = C(n; s, \mu, \sigma)$	Trajectories involving lane-changes in highD	Near-crashes in 100-Car NDS	1) is no less conflict-indicative than any of PSD, DRAC, and TTC; 2) is generalisable across datasets.
Conflict intensity evaluation $n = C^{-1}(p; s, \mu, \sigma)$	Trajectories involving lane-changes in highD	Lane-changes in highD	1) covers more diverse conflicts during lane-changes than TTC; 2) detects conflicts in a long-tailed distribution of intensity.

4.1 Data and experiment details

We use two naturalistic trajectory datasets in this study. First is the highD dataset that was collected at 6 different locations on German highways using drones (Krajewski et al. 2018). It includes detailed information about vehicle types, sizes, and movements, with a positioning error typically less than 10 cm. Considering that a significant part of driving on highways is independent without interactions with other vehicles, we select trajectories that involve lane-changes in highD. In addition to the high-quality drone-collected data for model training, a dataset of real-world conflicts is necessary for demonstration. The second dataset we use is from the 100-Car Naturalistic Driving Study (NDS), which is an instrumented-vehicle study conducted in the U.S. over 2 years in the early 2000s (Dingus et al. 2006). An event database (Custer 2018) resulted from the study compiles information on 68 crashes and 760 near-crashes. From the time-series sensor data of radars and accelerometers, we reconstruct bird’s eye view trajectories for these events². Due to missing values, inaccuracy of sensing, and the lack of ground truth, not all of the events can be reconstructed. We end up matching 180 events based on the restriction of insufficient space (distance less than 4.5 m) for undetected vehicles, including 11 crashes and 169 near-crashes as summarised in Table 3.

²We open-source our trajectory reconstruction code at <https://github.com/Yiru-Jiao/Reconstruct100CarNDSData>

Table 3. Summary of matched and selected events in 100-Car NDS data.

Event happened with	Matched crashes	Matched near-crashes	Selected near-crashes
leading vehicle	5	119	47
following vehicle	6	30	17
vehicle in adjacent lane	0	13	2
vehicle turning across oncoming traffic	0	4	0
vehicle crossing through an intersection	0	2	0
vehicle in oncoming traffic	0	1	0
In total	11	169	66

The first experiment estimates conflict probability at each time moment for the events in 100-Car NDS data. We utilise the estimation to issue collision warnings, and compare warning effectiveness with using 3 other commonly used surrogate metrics. Effective collision warning maximises true positives while minimising false positives. To reserve safe interactions within an event, we select events with a duration of at least 6 seconds, no hard braking (acceleration larger than -1.5 m/s^2) in the first 3 seconds, and speeds larger than 3 m/s at the first time moment for both vehicles involved. After the selection, 4 crashes and 66 near-crashes remained. Considering the relatively low reliability of data in crashes and for a consistent comparison, we use only the selected near-crashes, which are also shown in Table 3. The 3 broadly used metrics for comparison are Proportion of Stopping Distance (PSD), Deceleration Rate to Avoid a Crash (DRAC), and Time-to-Collision (TTC). Table 4 provides an overview of them, where Δs is the distance between vehicle bounding boxes and Δv is relative velocity. For PSD we use a braking rate of 5.5 m/s^2 , as emergency braking is typically between 1.6 and 5.5 m/s^2 (Fambro et al. 2000; Deligianni et al. 2017).

Table 4. Existing surrogate metrics of conflicts that are used for warning comparison.

Metric	Calculation	Note	Reference(s)	Proximity s	Context θ
PSD	$\frac{\Delta s}{v_{\text{follower}}^2/2/\text{dec}}$	dec = 5.5 m/s^2	(Allen et al. 1978)	Δs	v_{follower}^2
DRAC	$\frac{\ \Delta v\ ^2}{2\Delta s}$	approaching only	(D. F. Cooper and Ferguson 1976)	Δs	$\ \Delta v\ ^2$
TTC	$\frac{\Delta s}{\ \Delta v\ }$	approaching only	(Hayward 1972; Hydén 1987)	Δs	$\ \Delta v\ $

The second experiment evaluates conflict intensity at each time moment for lane-change interactions in the highD dataset. We use lane-changes to demonstrate the applicability of our unified metric to two-dimensional conflicts, which remain challenging to be integratively indicated by traditional metrics. We identify lane changes using the lane references provided in highD data. Then we determine the start and end moments of a lane-change based on the time when the vehicle deviates 1/3 of its vehicle width from the centerline of its current lane. In this way, overtaking is considered as two consecutive lane-changes. Seeing the vehicle making a lane-change as an ego vehicle, the lane-change is potentially interactive if there is a vehicle in front or at rear of the ego vehicle in either the original lane or the target lane. Then we use both the unified metric and two-dimensional TTC (2D-TTC) to evaluate conflict intensity (if any) at each time moment. Here 2D-TTC follows the typical definition of TTC, assuming constant velocities for two approaching vehicles at the moment of evaluation³. The smaller the TTC value, the higher the conflict intensity; when TTC is infinite, no potential collision is expected to occur.

In both experiments, we use a single unified metric trained with the trajectories involving lane-changes in highD data. In this way, the first experiment can additionally demonstrate the generalisability of our methodology; and the metric thresholds calibrated with real-world near-crashes can be used in the second experiment to distinguish conflicts. For a fair comparison with existing metrics, we avoid complex representations for interaction context θ . Firstly, we include the information used in PSD, DRAC, and TTC, i.e., v_{follower}^2 , $\|\Delta v\|^2$, and $\|\Delta v\|$ as analysed in Table 4. Since the lead-follow relationship evolves during lane-changing, we use the squared speeds of both ego vehicles (which change

³We open-sourced an algorithm for fast computation of two-dimensional TTC at <https://github.com/Yiru-Jiao/Two-Dimensional-Time-To-Collision>. This algorithm is used for all experiments in this study.

lanes) and target vehicles (in the surroundings). Further, we consider the accelerations of ego vehicles⁴, heading directions of target vehicles relative to their ego vehicles, and lengths of both ego and target vehicles. In order to indicate two-dimensional conflicts, we define proximity s utilising the two-dimensional spacing proposed in (Jiao et al. 2023). This spacing is denoted by (x, y) in the real-time transformed relative coordinate systems, and we convert (x, y) into (ρ, s) into polar coordinate systems, where ρ is the angle between (x, y) and $(1, 0)$ with a range of $[-\pi, \pi]$. Then we add ρ as one more variable in θ , and use s as the proximity measure to reflect conflict hierarchy.

We train two sets of SVGP models under different settings of the hyper-parameter β in Equation (13), with $\beta = 5$ and $\beta = 10$. Our training is on 60% of the selected interaction trajectories involving lane-changes; and the validation set and test set account for 20% each. During the training, we reduce the learning rate dynamically to avoid overfitting of the models, and stop training early when validation loss converges. Figure 4 shows the training progress, where there are 271 batches per epoch and 2,048 samples per batch. Training in both settings converges well, and stops earlier as well as reaches lower loss values when $\beta = 5$. We then evaluate model performance by both loss and negative log-likelihood (NLL) on validation and test sets, as presented in Figure 4. As a result, we select the model achieving the minimum test loss and the second minimum test NLL, i.e., the model with $\beta = 5$ after 52 epochs of training, to apply in the subsequent demonstration experiments.

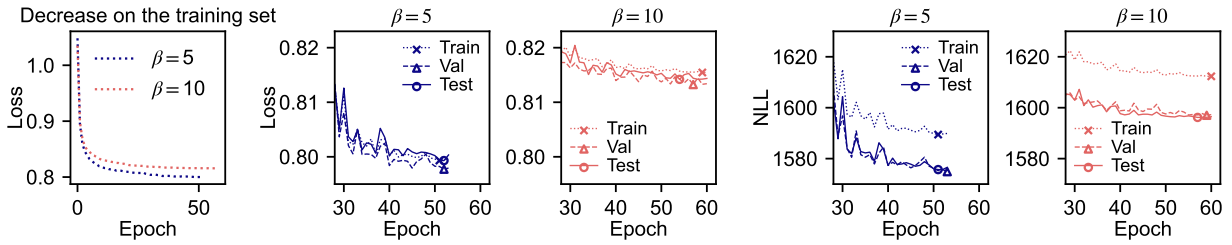


Figure 4. Evaluation of SVGP training and selection of the model to apply.

Since we consider two-dimensional interactions, maintaining a consistent coordinate system is necessary. The highD dataset uses a coordinate system where the x-axis points from left to right and the y-axis points downwards. This is a mirrored system from the traditional engineering coordinate system where the y-axis points upwards. When applying a model that is trained on highD data to other datasets, such as the 100-Car dataset, it is essential to adjust for this inconsistency. We make adjustments by exchanging the x and y coordinates of positions, velocities, and heading directions in 100-Car NDS data before coordinate transformation. We hereby remind the readers to correct potential inconsistencies in the coordinate systems between training data and application data.

4.2 Collision warning compared with existing metrics

The first experiment based on conflict probability estimation is designed to demonstrate two characteristics of our methodology. First, the unified metric performs at least as well as any among PSD, DRAC, and TTC in collision warning. This is determined in theory, but experimental results with real-world near-crashes can provide additional evidence. Second, we trained the unified metric with trajectories in the highD dataset while applying it to the events in 100-Car NDS data. This cross-validation involves not only the differences between German and American driving, but also the evolution of driving over more than 15 years. If the highD-trained metric performs well for 100-Car near-crashes, we can argue for the generalisability of this methodology, which implies common principles in human road use interactions.

In order to systematically compare warning effectiveness, we define performance indicators as explained in Table 5. Collision warning classifies safe and unsafe interactions based on the values and specific thresholds of metrics. Seeing the metrics as different classification models, we can compare their ROC curves, and a metric is better if the area under its curve is larger. For each metric, we then select an optimal threshold such that the corresponding point on their ROC curve is closest to the ideal point with zero false positive and all true positives (0%, 100%). Based on the optimal threshold, we further calculate warning periods and warning timeliness. The warning period of an event should ideally be close to 100%, but good warning timeliness does not necessarily mean early warning. On average, people need 1 to 1.3 seconds in response to an obstacle by braking, and in emergencies this can be less than 1 second (Summala 2000;

⁴We do not include target vehicle accelerations because this information is lacking in 100-Car NDS data and cannot be reliably derived due to speed fluctuations prior to potential collisions. This lack also prevents comparison with the metric Modified Time to Collision (MTTC).

Markkula et al. 2016). Therefore, good warning timeliness should not be too large, as it may distract people earlier than they need to be warned; neither should it be too small, as the best timing to prevent a potential collision may be missed.

Table 5. Definitions of the performance indicators for collision warning effectiveness comparison.

Performance indicator	Definition
True positive	The first 3 seconds in each of the selected events are supposed to be safe, so any warning in this period marks a false positive.
False positive	Seeing the moment when conflicting vehicles reach the minimum distance as a critical moment, the 3 seconds prior to the moment are supposed to be dangerous; any warning in this period marks a true positive.
True positive rate and false positive rate (%)	The rate of true positives and false positives, respectively, among all events. True positive rate ideally approximates 100% and false positive rate 0%.
ROC curve	Receiver Operating Characteristic curve that plots true positive rate against false positive rate at various thresholds.
Warning period (%)	For each event with warnings issued under the optimal threshold, the percentage of warned time moments within the annotated conflict period.
Warning timeliness (s)	For each event with warnings issued under the optimal threshold, the time interval from the last safe-unsafe shift of warning until the critical moment.

Figure 5 presents the comparison of collision warning effectiveness. In the plot of ROC curves, we use circles centred at the ideal point (0%, 100%) and crossing the optimal points of different metrics to facilitate comparing their closeness to the ideal point. The metrics of DRAC, TTC, and Unified have comparable areas under their ROC curves, while PSD is less effective. Zooming in to see more details at the top left corner, TTC and Unified are consistently better than DRAC, and are very close to the ideal point. More specifically, the optimal threshold of Unified is $n^* = 17$, reaching a true positive rate of 95.45% and a false positive rate of 4.55%; $TTC^* = 4.2$ s and achieves 93.94% true positive rate and 0.00% false positive rate; $DRAC^* = 0.45$, with a true positive rate of 92.42% and a false positive rate of 7.58%. Much less comparably, the optimal threshold of PSD is 0.52, with a true positive rate of 57.58% only but a false positive rate of 25.76%.

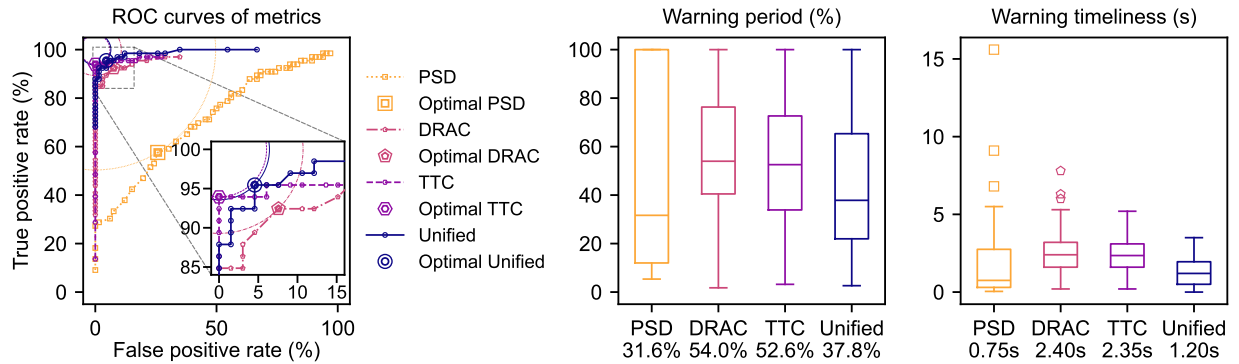
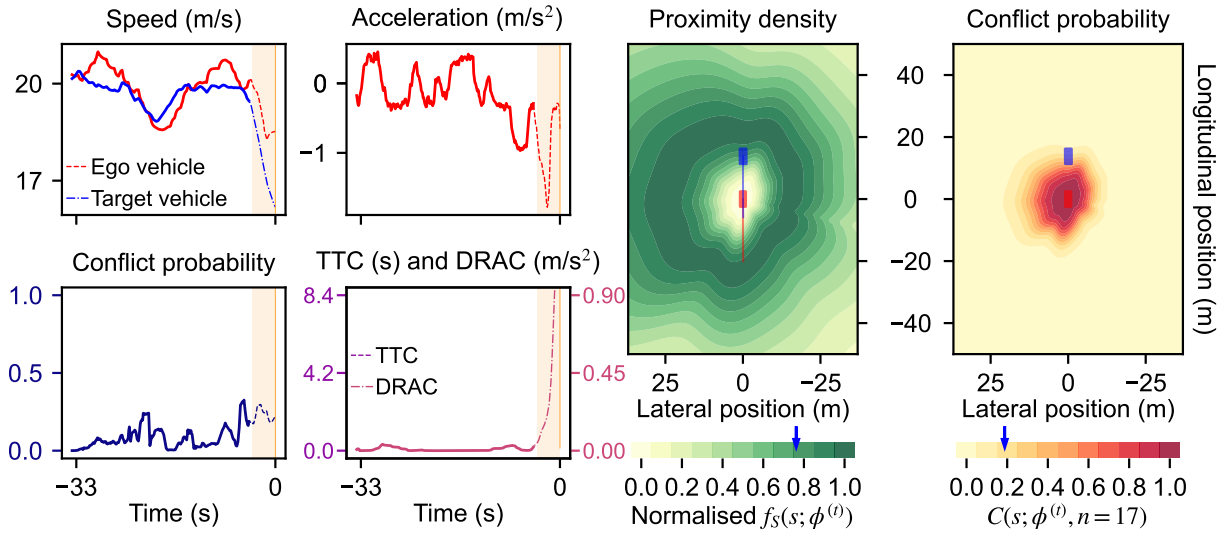


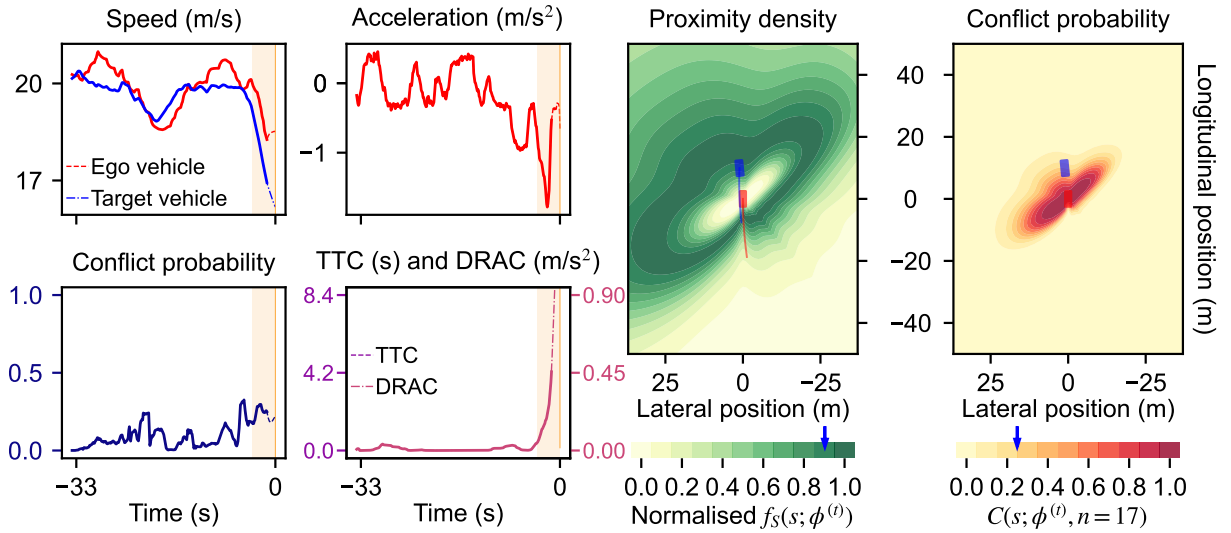
Figure 5. Collision warning effectiveness comparison between PSD, DRAC, TTC, and Unified. In the boxplots of warning period and timeliness, median values are marked below the labels of metrics.

These metrics are further compared at their optimal thresholds by the box plots of warning period and warning timeliness in Figure 5. Given the weak effectiveness of PSD, its warning period and timeliness are not comparable with other metrics. Both DRAC and TTC have higher median warning periods than Unified. This suggests that the unified metric may not issue a warning at the beginning of the annotated conflicts. This is also verified in the plot of warning timeliness, where DRAC and TTC have similar distributions and their median timeliness is both earlier than that of Unified. In addition, the warning timeliness of Unified is less varied. From a positive perspective, this means that using the unified metric gives consistent warnings and does not distract drivers too much; whereas from a negative perspective, this means that the unified metric may miss the chance to prevent a potential collision.

For a more detailed analysis, Figure 6 shows two frames in the trip indexed by 8332. This event is warned by DRAC only, while TTC is larger than 10.59 s throughout and the conflict probability estimated by Unified remains lower than 0.5. In this figure, we present the profiles of speed, acceleration, and metric values, with the annotated conflict period shaded. We also plot heatmaps of proximity density distribution $f(s; \phi)$ and conflict probability function $C(s; \phi, n)$, where the y-axis points to the heading direction of ego vehicle and the x-axis points from right to left to align with highD's coordinate system. For each location around the ego vehicle, we assume the target vehicle is at that location and use actual interaction context θ for estimation. Figure 6a is the frame at 4.4 seconds before the critical moment; and Figure 6b is 1.4 seconds before. Notably, in Figure 6b, the proximity density distribution, i.e., probable positions of the target vehicle given the interaction context $\phi^{(t)}$, does not point to the ego vehicle's heading direction. This is due to the lateral interaction between these two vehicles, which is in line with the narrative data of this event: the target vehicle was merging into the right lane ahead of the ego vehicle, causing the ego vehicle to brake to avoid a collision. Comparing the two frames, the unified metric takes into account the ego vehicle's deceleration as successful prevention of an immediate conflict, and thus the conflict probability stays low during the annotated conflict period.



(a) Frame 4.4 seconds prior to the critical moment of trip 8332.



(b) Frame 1.4 seconds prior to the critical moment of trip 8332.

Figure 6. Visualisation example for the collision warning of trip 8332.

We summarise the success and failure cases of conflict warnings in Table 6. PSD is not included due to its lower effectiveness. For the events where at least one of Unified, TTC, and DRAC fails, as well as for the false warnings of Unified, we provide dynamic visualisations along with our open-sourced code. The readers are referred to the Acknowledgements to find links. Impressively, 58 out of the 61 near-crashes are correctly warned by all the metrics of Unified, TTC, and DRAC. This is because most events in the 100-Car dataset are rear-end conflicts during car following, for which TTC and DRAC have been proven to be useful. In the next experiment, TTC and our unified metric are challenged to handle two-dimensional traffic conflicts.

Table 6. Summary of success and failure cases of collision warnings by Unified, TTC, and DRAC.

Unified	TTC	DRAC	Number of events	Trip ID
Succeed	Succeed	Succeed	58	
Succeed	Succeed	Fail	3	8622, 8854, 9101
Succeed	Fail	Succeed	0	
Succeed	Fail	Fail	2	8463, 8810
Fail	Succeed	Succeed	1	8761
Fail	Succeed	Fail	0	
Fail	Fail	Succeed	2	8332, 8702
Fail	Fail	Fail	0	

4.3 Conflict intensity evaluation for lane-changing interactions

The second experiment evaluates the conflict intensity of lane-changing interactions, with which we want to demonstrate two more characteristics of our methodology. First, this methodology can cover a more diverse range of conflicts during lane-changes than TTC. This stands in theory because TTC assumes constant movements (velocities in this study) of interacting vehicles, which identifies potential lane-change conflicts only if two vehicles have crossing velocity directions and could collide without movement change. In contrast, a unified metric trained with our methodology on two-dimensional daily driving data considers conflicts in all directions and varying interaction situations. Second, the intensity of conflicts evaluated by this methodology is expected to have a long-tailed distribution. More specifically, the number of detected conflicts should decrease according to a power-law as conflict intensity increases. A long tail in such a distribution indicates that, although high-intensity conflicts are extremely rare, they occur with a non-negligible probability. Not all surrogate metrics of conflicts have this characteristic, but it is crucial not to ignore very rare conflicts.

There are 13,364 lane-changes in the highD dataset, and in total 713 (5.34%) of the lane-changes involve at least 1 second consecutively identified as a conflict by either TTC or the unified metric. This identification is under the optimal thresholds found in the first experiment, i.e., of 4.2 s for TTC and 17 for Unified. Among these lane-changes, in 679 the ego vehicle conflicts with one other vehicle, in 31 the ego vehicle conflicts with 2 other vehicles, and in 3 the ego vehicle conflicts with 3 other vehicles. These constitute 750 conflicts, among which 67 are indicated by both TTC and Unified; 18 are indicated by TTC only; and 665 are indicated by Unified only. In Figure 7, we plot the scattered relative locations of target vehicles to their ego vehicles aggregated at (0, 0). These locations are where a lane-changing interaction reaches the minimum TTC or the maximum intensity evaluated by Unified.

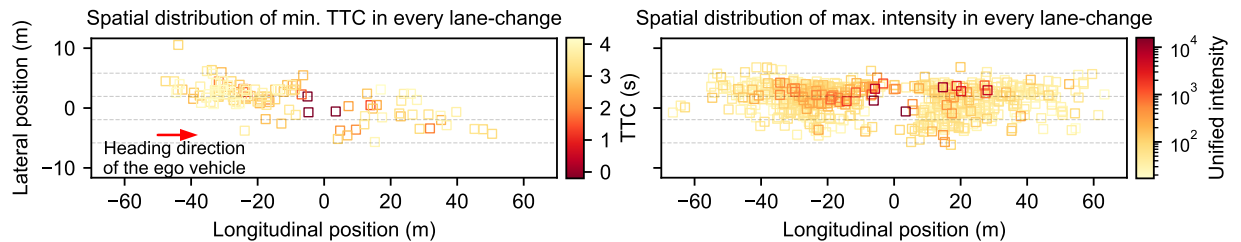


Figure 7. Spatial distributions of conflict moments with minimum TTC or maximum intensity in every lane-change. Target vehicle positions are transformed to a coordinate system centred at the ego vehicle position and with the longitudinal axis pointing to the ego vehicle heading direction. The dashed lines mark lanes at the average lane width in highD data.

Figure 7 clearly shows that conflict detection by TTC strongly relies on the assumption of constant movements, while training a unified metric can cover all directions around the ego vehicle and accounts for the heterogeneity of proximity behaviour in every different direction. There are significantly more conflicts between the ego vehicles making lane-changes and the target vehicles in the left lane than those in the right lane. This may be due to more lane-changes from right to left or higher speeds of vehicles on the left lane, but future investigation is needed for more precise reasons. Notably, most of the lane-changing interactions have intensities lower than 100, which means one such conflict on average occurs in every 100 or fewer interactions. In comparison, conflicts with intensities higher than 100 are fewer, and those with intensities higher than 1000 are significantly fewer. However, despite their seeming rarity, they are far from unlikely to occur. In fact, foreseeing and preventing these safety-critical events remain key challenges for safe driving (Liu and Feng 2024).

A closer look at the intensity distribution is presented with Figure 8. In the left half of the figure, we plot the histograms of TTC values and Unified intensities respectively, for those at each individual moment and for averaged during each lane-change conflict. The averaged values consider only lane-changing process, while the individual moments include car-following periods before and after lane-changes. The histograms show a decreasing frequency when intensity increases (TTC decreases), which is aligned with the assumption of conflict hierarchy. To further see if the distributions are long-tailed, in the right half of Figure 8, we make log-log scatter plots of the distributions, as well as their dashed trend lines and calibrated functions. All of the logarithm relationships are linear, therefore, all distributions to different extents have the characteristic of power-law. However, the trend line of TTC values averaged during lane-change conflicts has a higher slope than the line of TTC values at individual moments. This suggests that TTC detects fewer lane-changing conflicts than car-following conflicts. In contrast, the unified metric evaluates conflicts in the same theoretical framework, and thus has more consistent trend lines between averaging during lane-changes and at individual moments.

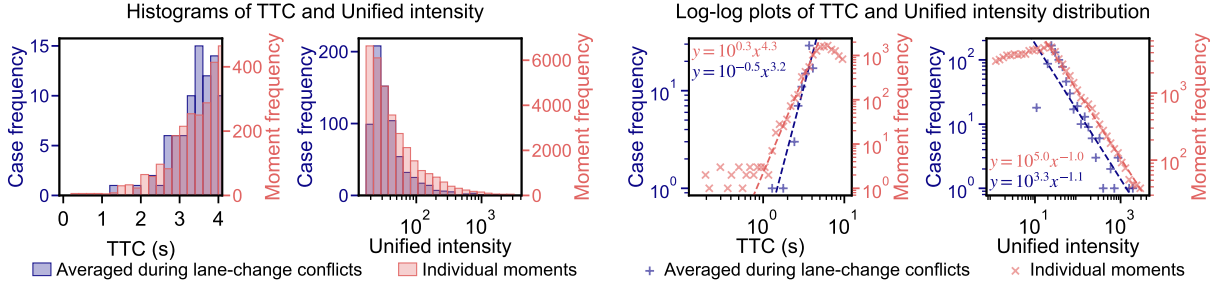
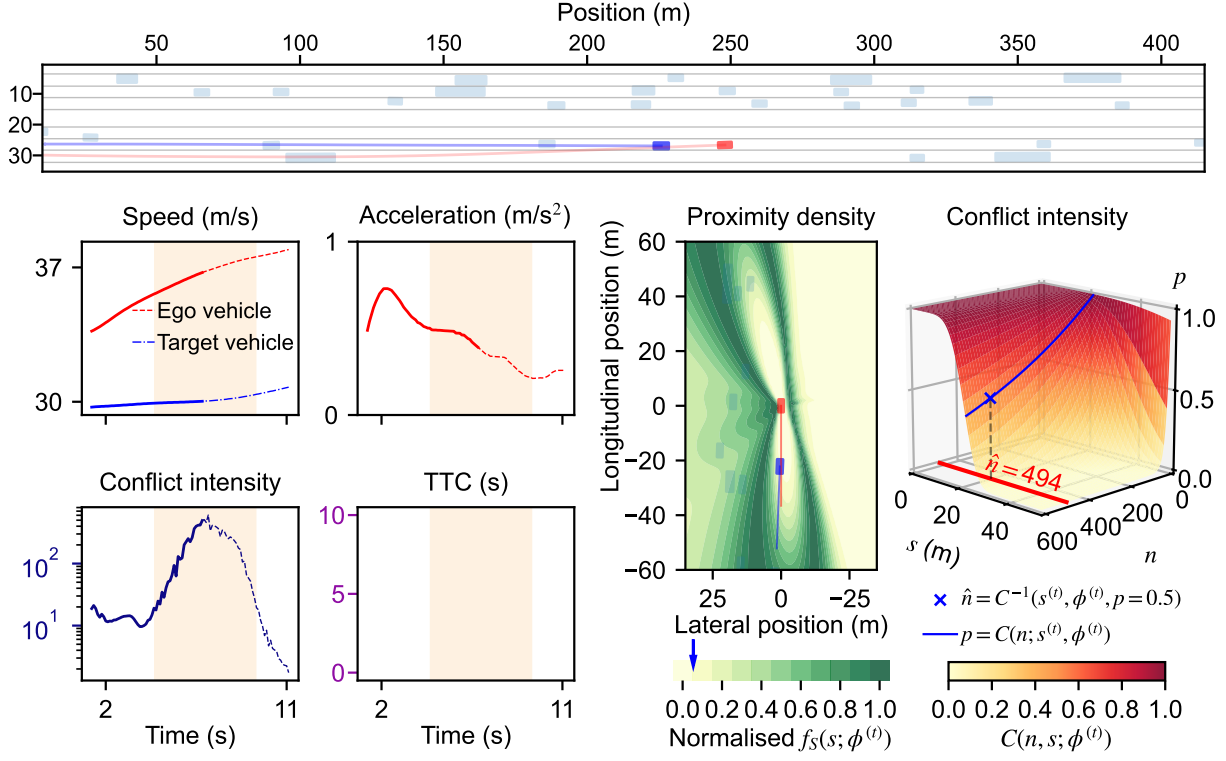


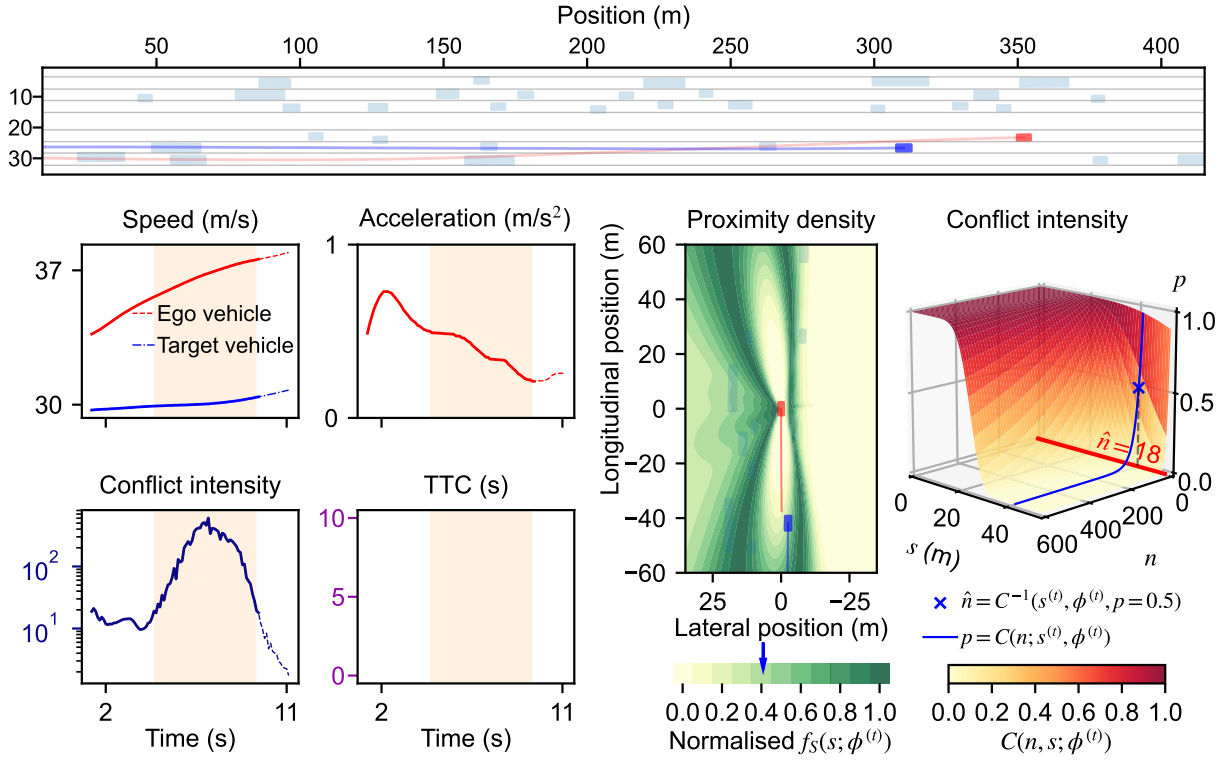
Figure 8. Intensity distributions during lane-changing interactions and at all individual moments in the highD dataset.

To provide more intuitive information, we make dynamic visualisations for the detected conflicts in different ranges of intensity indicated by TTC and Unified. A link can be found in the Acknowledgements. Here in Figure 9 we present an example at location 1 with vehicle track indices of 1860 and 1858. The ego vehicle in red makes two sequential lane-changes, and conflicts with the target vehicle in the intermediate lane. Similar to the visualisation for near-crashes in Section 4.2, we plot the profiles of speed, acceleration, evaluated conflict intensity, and TTC values, as well as a real-time heatmap of proximity distribution. In the plots of profiles, lane-change periods are shaded. In addition, we visualise the surface of conflict detection $C(n; s; \phi)$, which relates conflict intensity n , current proximity s , and conflict probability p .

The first frame in Figure 9a is when the ego vehicle finishes its first lane-change from the right lane to the middle lane. In this frame, the conflict intensity is evaluated to reach the highest level during the whole process of sequential lane-changes. On the surface of conflict detection, we plot a line showing the relationship between conflict intensity and probability at real-time proximity. This moment is at a very high probability to be considered as a minor conflict, and the maximum intensity to be considered as a conflict, i.e., the maximum intensity if conflict probability is larger than 0.5, reaches 494. Then the evaluated intensity decreases when the ego vehicle leaves the middle lane and continues moving to the left lane. In the frame shown in Figure 9b, at the end of these two sequential lane changes, the evaluated intensity returns to safe levels.



(a) Frame 9719 at which the ego vehicle finishes first lane-change from the right lane to the middle lane.



(b) Frame 9747 at which the ego vehicle changes lane again to the left lane.

Figure 9. Example dynamic visualisation of a lane-changing conflict detected by Unified only.

5 Conclusion and discussion

Conflicts do not arise out of nowhere, and every conflict is a continuation of preceding safe interactions. Based on this assumption, this study first introduces a unified theory of traffic conflicts, and then proposes a statistical learning approach that applies the theory to conflict detection. Our experiments on conflict probability estimation and conflict intensity evaluation use real-world data and train a unified metric based on the proposed theory and through the learning approach. Experiment results demonstrate that the unified metric provides effective collision warnings, is generalisable across datasets, covers various conflicts consistently, and detects conflicts in a long-tailed distribution of intensity. These features enable consistent conflict detection and safety evaluation, implying significant research opportunities. For example, proximity-based surrogate metrics of conflicts can be integrated into a single theoretical framework; with the statistical learning approach, more effective surrogate metrics can be learned from data; given that collision risk can be consistently evaluated in varying situations, it is possible to compare road user interactions in different situations and thus provide consistent assessment on the safety of road infrastructures; furthermore, combining the generalisability and detection ability of high-intensity conflicts, safety-critical events that are never observed in training data may be effectively identified, reinforced, and generated.

The current study has several limitations, which can be investigated in future research.

- The proposed theory is not able to directly anticipate when a collision will happen. This can be addressed by incorporating trajectory prediction models and forming a more comprehensive framework for safe interaction planning.
- This theory is based on proximity and does not indicate the severity of a potential collision. Collision severity estimation focuses on the energy released by a collision, which is not extreme value theory based, but more physics driven. Severity is an important aspect of collision avoidance, therefore, more exploration is required.
- We use spatial proximity and trajectory datasets of vehicles for demonstration in this study, while the theory can be applied to temporal proximity and the statistical learning can involve multiple categories of road users including pedestrians and cyclists. Future research on multi-modal interaction safety is thus promising.
- The uncertainty of conflict probability estimation and conflict intensity evaluation is not quantified in this study. Such quantification can inform the reliability of conflict detection. This can be achieved by inferring the distributions of proximity characteristic parameters, which is theoretically feasible as the parameters are learned based on Gaussian.

Importantly, although we explained learning the representation of interaction context as a key task, this study does not conduct representation learning. Theoretically, the statistical learning approach can include almost all the information one can collect to describe the interactions between road users. This can go beyond movements, including road layouts, weather, individual characteristics of road users, etc. It needs to be noted, however, that the more information gets involved, the more diverse data is required to train an effective unified metric. Given that the theory is suitable for learning from accumulative evidence, more research can be expanded upon continual learning, which is of interest to both the fields of traffic safety and autonomous driving.

Acknowledgments

This work is supported by the TU Delft AI Labs programme. We thank Dr. Haneen Farah for her insightful discussion and internal review. We also would like to thank the editor and anonymous reviewers for their valuable comments and advice.

We open-source our code for applying the methodology and repeating our experiments at <https://github.com/Yiru-Jiao/UnifiedConflictDetection>. Dynamic visualisations of near-crashes in 100-Car NDS data are in the subfolder `./Data/DynamicFigures/ProbabilityEstimation/gifs/`; of lane-changing conflicts in highD data in the subfolder `./Data/DynamicFigures/IntensityEvaluation/gifs/`.

References

- Abdel-Aty, M., Z. Wang, O. Zheng, and A. Abdelraouf (2023). “Advances and applications of computer vision techniques in vehicle trajectory generation and surrogate traffic safety indicators”. In: *Accident Analysis & Prevention* 191, p. 107191. DOI: [10.1016/j.aap.2023.107191](https://doi.org/10.1016/j.aap.2023.107191).
- Allen, B. L., B. T. Shin, and P. J. Cooper (1978). “Analysis of Traffic Conflicts and Collisions”. In: *Transportation Research Record* (667), pp. 67–74.

- Anwari, N., M. Abdel-Aty, A. Goswamy, and O. Zheng (2023). “Investigating surrogate safety measures at midblock pedestrian crossings using multivariate models with roadside camera data”. In: *Accident Analysis & Prevention* 192, p. 107233. DOI: [10.1016/j.aap.2023.107233](https://doi.org/10.1016/j.aap.2023.107233).
- Arun, A., M. M. Haque, A. Bhaskar, S. Washington, and T. Sayed (2021). “A systematic mapping review of surrogate safety assessment using traffic conflict techniques”. In: *Accident Analysis & Prevention* 153, p. 106016. DOI: [10.1016/j.aap.2021.106016](https://doi.org/10.1016/j.aap.2021.106016).
- Arun, A., M. M. Haque, S. Washington, T. Sayed, and F. Mannering (2021). “A systematic review of traffic conflict-based safety measures with a focus on application context”. In: *Analytic Methods in Accident Research* 32, p. 100185. DOI: [10.1016/j.amar.2021.100185](https://doi.org/10.1016/j.amar.2021.100185).
- Beitel, D., J. Stipanovic, K. Manaugh, and L. Miranda-Moreno (2018). “Assessing safety of shared space using cyclist-pedestrian interactions and automated video conflict analysis”. In: *Transportation Research Part D: Transport and Environment* 65, pp. 710–724. DOI: [10.1016/j.trd.2018.10.001](https://doi.org/10.1016/j.trd.2018.10.001).
- Borsos, A., H. Farah, A. Lareshyn, and M. Hagenzieker (Aug. 2020). “Are collision and crossing course surrogate safety indicators transferable? A probability based approach using extreme value theory”. In: *Accident Analysis & Prevention* 143, p. 105517. DOI: [10.1016/j.aap.2020.105517](https://doi.org/10.1016/j.aap.2020.105517).
- Broadhurst, A., S. Baker, and T. Kanade (2005). “Monte Carlo road safety reasoning”. In: *Proceedings of IEEE Intelligent Vehicles Symposium*. DOI: [10.1109/ivs.2005.1505122](https://doi.org/10.1109/ivs.2005.1505122).
- Camara, F. and C. Fox (2020). “Space Invaders: Pedestrian Proxemic Utility Functions and Trust Zones for Autonomous Vehicle Interactions”. In: *International Journal of Social Robotics*. DOI: [10.1007/s12369-020-00717-x](https://doi.org/10.1007/s12369-020-00717-x).
- Chauhan, R., A. Dhamaniya, and S. Arkatkar (2022). “Challenges in Rear-end Conflict-based Safety Assessment of Highly Disordered Traffic Conditions”. In: *Transportation Research Record* 2677.2, pp. 624–634. DOI: [10.1177/03611981221108156](https://doi.org/10.1177/03611981221108156).
- Cooper, D. F. and N. Ferguson (1976). “Traffic studies at T-Junctions – A conflict simulation Record”. In: *Traffic Engineering & Control* 17 (7), pp. 306–309.
- Cooper, P. (Sept. 1977). “Reports from group discussions”. In: *Proceedings of the first workshop on traffic conflicts*. Oslo.
- Custer, K. (2018). *100-Car Data*. DOI: [10.15787/vtt1/ceu6rb](https://doi.org/10.15787/vtt1/ceu6rb).
- Das, L. C. and M. Won (2021). “SAINT-ACC: Safety-Aware Intelligent Adaptive Cruise Control for Autonomous Vehicles Using Deep Reinforcement Learning”. In: *Proceedings of the 38th International Conference on Machine Learning*. Ed. by M. Meila and T. Zhang. Vol. 139, pp. 2445–2455.
- Das, S. and A. K. Maurya (Dec. 2020). “Defining Time-to-Collision Thresholds by the Type of Lead Vehicle in Non-Lane-Based Traffic Environments”. In: *IEEE Transactions on Intelligent Transportation Systems* 21.12, pp. 4972–4982. DOI: [10.1109/tits.2019.2946001](https://doi.org/10.1109/tits.2019.2946001).
- Das, T., M. S. Samandar, and N. Roupail (2022). “Longitudinal traffic conflict analysis of autonomous and traditional vehicle platoons in field tests via surrogate safety measures”. In: *Accident Analysis & Prevention* 177, p. 106822. DOI: [10.1016/j.aap.2022.106822](https://doi.org/10.1016/j.aap.2022.106822).
- de Ceunynck, T. (2017). “Defining and applying surrogate safety measures and behavioural indicators through site-based observations”. PhD thesis. Transport and Roads, Hasselt University.
- Deligianni, S. P., M. Quddus, A. Morris, A. Anuur, and S. Reed (2017). “Analyzing and Modeling Drivers’ Deceleration Behavior from Normal Driving”. In: *Transportation Research Record* 2663.1, pp. 134–141. DOI: [10.3141/2663-17](https://doi.org/10.3141/2663-17).
- Dingus, T. A., S. G. Klauer, V. L. Neale, A. Petersen, S. E. Lee, J. Sudweeks, M. A. Perez, J. Hankey, D. Ramsey, S. Gupta, and C. Bucher (2006). *The 100-car naturalistic driving study, Phase II-Results of the 100-car field experiment DOT-HS-810-593*. Tech. rep. United States. Department of Transportation. National Highway Traffic Safety Administration.
- Fambro, D. B., R. J. Koppa, D. L. Picha, and K. Fitzpatrick (2000). “Driver Braking Performance in Stopping Sight Distance Situations”. In: *Transportation Research Record* 1701.1, pp. 9–16. DOI: [10.3141/1701-02](https://doi.org/10.3141/1701-02).
- Farah, H. and C. L. Azevedo (Apr. 2017). “Safety analysis of passing maneuvers using extreme value theory”. In: *IATSS Research* 41.1, pp. 12–21. DOI: [10.1016/j.iatssr.2016.07.001](https://doi.org/10.1016/j.iatssr.2016.07.001).
- Formosa, N., M. Quddus, S. Ison, M. Abdel-Aty, and J. Yuan (2020). “Predicting real-time traffic conflicts using deep learning”. In: *Accident Analysis & Prevention* 136, p. 105429. DOI: [10.1016/j.aap.2019.105429](https://doi.org/10.1016/j.aap.2019.105429).
- Gardner, J., G. Pleiss, K. Q. Weinberger, D. Bindel, and A. G. Wilson (2018). “GPYtorch: Blackbox Matrix-Matrix Gaussian Process Inference with GPU Acceleration”. In: *Advances in Neural Information Processing Systems*. Ed. by S. Bengio, H. Wallach, H. Larochelle, K. Grauman, N. Cesa-Bianchi, and R. Garnett. Vol. 31.
- Hayward, J. C. (1972). “Near miss determination through use of a scale of danger”. In: *51st Annual Meeting of the Highway Research Board*, pp. 24–34.
- Hydén, C. (1987). “The development of a method for traffic safety evaluation: The Swedish Traffic Conflicts Technique”. PhD thesis. Lund University.

- Jankowiak, M., G. Pleiss, and J. Gardner (July 2020). "Parametric Gaussian Process Regressors". In: *Proceedings of the 37th International Conference on Machine Learning*. Ed. by H. D. III and A. Singh. Vol. 119, pp. 4702–4712.
- Jiao, Y., S. C. Calvert, S. van Cranenburgh, and H. van Lint (2023). "Inferring vehicle spacing in urban traffic from trajectory data". In: *Transportation Research Part C: Emerging Technologies* 155, p. 104289. DOI: [10.1016/j.trc.2023.104289](https://doi.org/10.1016/j.trc.2023.104289).
- Junietz, P., F. Bonakdar, B. Klamann, and H. Winner (2018). "Criticality Metric for the Safety Validation of Automated Driving using Model Predictive Trajectory Optimization". In: *2018 21st International Conference on Intelligent Transportation Systems (ITSC)*, pp. 60–65. DOI: [10.1109/itsc.2018.8569326](https://doi.org/10.1109/itsc.2018.8569326).
- Kim, J. and D. Kum (2018). "Collision Risk Assessment Algorithm via Lane-Based Probabilistic Motion Prediction of Surrounding Vehicles". In: *IEEE Transactions on Intelligent Transportation Systems* 19.9, pp. 2965–2976. DOI: [10.1109/tits.2017.2768318](https://doi.org/10.1109/tits.2017.2768318).
- Krajewski, R., J. Bock, L. Kloeker, and L. Eckstein (Nov. 2018). "The highD Dataset: A Drone Dataset of Naturalistic Vehicle Trajectories on German Highways for Validation of Highly Automated Driving Systems". In: *IEEE 21st International Conference on Intelligent Transportation Systems (ITSC)*. Maui, HI, United States, pp. 2118–2125. DOI: [10.1109/itsc.2018.8569552](https://doi.org/10.1109/itsc.2018.8569552).
- Kuang, Y., X. Qu, and S. Wang (2015). "A tree-structured crash surrogate measure for freeways". In: *Accident Analysis & Prevention* 77, pp. 137–148. DOI: [10.1016/j.aap.2015.02.007](https://doi.org/10.1016/j.aap.2015.02.007).
- Kusano, K. D., R. Chen, J. Montgomery, and H. C. Gabler (Sept. 2015). "Population distributions of time to collision at brake application during car following from naturalistic driving data". In: *Journal of Safety Research* 54, 95.e29–104. DOI: [10.1016/j.jsr.2015.06.011](https://doi.org/10.1016/j.jsr.2015.06.011).
- Laureshyn, A., Å. Svensson, and C. Hydén (2010). "Evaluation of traffic safety, based on micro-level behavioural data: Theoretical framework and first implementation". In: *Accident Analysis & Prevention* 42.6, pp. 1637–1646. DOI: [10.1016/j.aap.2010.03.021](https://doi.org/10.1016/j.aap.2010.03.021).
- Lewis-Evans, B., D. De Waard, and K. A. Brookhuis (Nov. 2010). "That's close enough—A threshold effect of time headway on the experience of risk, task difficulty, effort, and comfort". In: *Accident Analysis & Prevention* 42.6, pp. 1926–1933. DOI: [10.1016/j.aap.2010.05.014](https://doi.org/10.1016/j.aap.2010.05.014).
- Li, Y., J. Lu, and K. Xu (2017). "Crash Risk Prediction Model of Lane-Change Behavior on Approaching Intersections". In: *Discrete Dynamics in Nature and Society* 2017, pp. 1–12. DOI: [10.1155/2017/7328562](https://doi.org/10.1155/2017/7328562).
- Liu, H. X. and S. Feng (2024). "Curse of rarity for autonomous vehicles". In: *Nature Communications* 15.1. DOI: [10.1038/s41467-024-49194-0](https://doi.org/10.1038/s41467-024-49194-0).
- Lu, C., X. He, H. van Lint, H. Tu, R. Happee, and M. Wang (Nov. 2021). "Performance evaluation of surrogate measures of safety with naturalistic driving data". In: *Accident Analysis & Prevention* 162, p. 106403. DOI: [10.1016/j.aap.2021.106403](https://doi.org/10.1016/j.aap.2021.106403).
- Mannering, F. L., V. Shankar, and C. R. Bhat (2016). "Unobserved heterogeneity and the statistical analysis of highway accident data". In: *Analytic methods in accident research* 11, pp. 1–16. DOI: [10.1016/j.amar.2016.04.001](https://doi.org/10.1016/j.amar.2016.04.001).
- Markkula, G., J. Engström, J. Lodin, J. Bärgman, and T. Victor (Oct. 2016). "A farewell to brake reaction times? Kinematics-dependent brake response in naturalistic rear-end emergencies". In: *Accident Analysis & Prevention* 95, pp. 209–226. DOI: [10.1016/j.aap.2016.07.007](https://doi.org/10.1016/j.aap.2016.07.007).
- Mazaheri, A., M. Saffarzadeh, N. Nadimi, and S. S. Naserlavi (2023). "A revise on using surrogate safety measures for rear-end crashes". In: *IATSS Research* 47.1, pp. 105–120. DOI: [10.1016/j.iatssr.2023.02.003](https://doi.org/10.1016/j.iatssr.2023.02.003).
- Meng, Q. and X. Qu (2012). "Estimation of rear-end vehicle crash frequencies in urban road tunnels". In: *Accident Analysis & Prevention* 48, pp. 254–263. DOI: [10.1016/j.aap.2012.01.025](https://doi.org/10.1016/j.aap.2012.01.025).
- Nadimi, N., A. M. Amiri, and A. Sadri (2021). "Introducing novel statistical-based method of screening and combining currently well-known surrogate safety measures". In: *Transportation Letters* 14.4, pp. 385–395. DOI: [10.1080/19427867.2021.1874184](https://doi.org/10.1080/19427867.2021.1874184).
- Nadimi, N., S. S. NaserAlavi, and M. Asadamraji (Dec. 2022). "Calculating dynamic thresholds for critical time to collision as a safety measure". In: *Proceedings of the Institution of Civil Engineers - Transport* 175.7, pp. 403–412. DOI: [10.1680/jtran.19.00066](https://doi.org/10.1680/jtran.19.00066).
- Panou, M. C. (June 2018). "Intelligent personalized ADAS warnings". In: *European Transport Research Review* 10.2. DOI: [10.1186/s12544-018-0324-6](https://doi.org/10.1186/s12544-018-0324-6).
- Pawar, D. S. and G. R. Patil (2016). "Critical gap estimation for pedestrians at uncontrolled mid-block crossings on high-speed arterials". In: *Safety Science* 86, pp. 295–303. DOI: [10.1016/j.ssci.2016.03.011](https://doi.org/10.1016/j.ssci.2016.03.011).
- Razi, A., X. Chen, H. Li, H. Wang, B. Russo, Y. Chen, and H. Yu (2022). "Deep learning serves traffic safety analysis: A forward-looking review". In: *IET Intelligent Transport Systems* 17.1, pp. 22–71. DOI: [10.1049/itr2.12257](https://doi.org/10.1049/itr2.12257).
- Reiss, R.-D. and M. Thomas (1997). *Statistical analysis of extreme values*. Basel, Switzerland: Birkhäuser.
- Saunier, N., N. Mourji, and B. Agard (2011). "Mining Microscopic Data of Vehicle Conflicts and Collisions to Investigate Collision Factors". In: *Transportation Research Record: Journal of the Transportation Research Board* 2237.1, pp. 41–50. DOI: [10.3141/2237-05](https://doi.org/10.3141/2237-05).

- Saunier, N., T. Sayed, and C. Lim (Sept. 2007). “Probabilistic Collision Prediction for Vision-Based Automated Road Safety Analysis”. In: *2007 IEEE Intelligent Transportation Systems Conference*. DOI: [10.1109/itsc.2007.4357793](https://doi.org/10.1109/itsc.2007.4357793).
- Schiff, W. and M. L. Detwiler (1979). “Information Used in Judging Impending Collision”. In: *Perception* 8.6, pp. 647–658. DOI: [10.1068/p080647](https://doi.org/10.1068/p080647).
- Siebert, F. W., M. Oehl, F. Bersch, and H.-R. Pfister (2017). “The exact determination of subjective risk and comfort thresholds in car following”. In: *Transportation Research Part F: Traffic Psychology and Behaviour* 46, pp. 1–13. DOI: [10.1016/j.trf.2017.01.001](https://doi.org/10.1016/j.trf.2017.01.001).
- Siebert, F. W., M. Oehl, and H.-R. Pfister (2014). “The influence of time headway on subjective driver states in adaptive cruise control”. In: *Transportation Research Part F: Traffic Psychology and Behaviour* 25, pp. 65–73. DOI: [10.1016/j.trf.2014.05.005](https://doi.org/10.1016/j.trf.2014.05.005).
- Songchitruksa, P. and A. P. Tarko (2006). “The extreme value theory approach to safety estimation”. In: *Accident Analysis & Prevention* 38.4, pp. 811–822. DOI: [10.1016/j.aap.2006.02.003](https://doi.org/10.1016/j.aap.2006.02.003).
- Summala, H. (Sept. 2000). “Brake Reaction Times and Driver Behavior Analysis”. In: *Transportation Human Factors* 2.3, pp. 217–226. DOI: [10.1207/sthf0203_2](https://doi.org/10.1207/sthf0203_2).
- Tageldin, A. and T. Sayed (2019). “Models to evaluate the severity of pedestrian-vehicle conflicts in five cities”. In: *Transportmetrica A: Transport Science* 15.2, pp. 354–375. DOI: [10.1080/23249935.2018.1477853](https://doi.org/10.1080/23249935.2018.1477853).
- Taieb-Maimon, M. and D. Shinar (2001). “Minimum and Comfortable Driving Headways: Reality versus Perception”. In: *Human Factors* 43.1, pp. 159–172. DOI: [10.1518/001872001775992543](https://doi.org/10.1518/001872001775992543).
- Tarko, A. P. (2018). “Surrogate measures of safety”. In: *Safe mobility: challenges, methodology and solutions*. Ed. by D. Lord and S. Washington. Vol. 11. Leeds: Emerald Publishing Limited, pp. 383–405. DOI: [10.1108/s2044-994120180000011019](https://doi.org/10.1108/s2044-994120180000011019).
- (2021). “A unifying view on traffic conflicts and their connection with crashes”. In: *Accident Analysis & Prevention* 158, p. 106187. DOI: [10.1016/j.aap.2021.106187](https://doi.org/10.1016/j.aap.2021.106187).
- Teigen, K. H. (2005). “The proximity heuristic in judgments of accident probabilities”. In: *British Journal of Psychology* 96.4, pp. 423–440. DOI: [10.1348/000712605x47431](https://doi.org/10.1348/000712605x47431).
- Uno, N., Y. Iida, S. Itsubo, and S. Yasuhara (2002). “A microscopic analysis of traffic conflict caused by lane-changing vehicle at weaving section”. In: *Proceedings of the 13th mini-EURO conference-handling uncertainty in the analysis of traffic and transportation systems*. Bari, Italy, pp. 10–13.
- Vahidi, A. and A. Eskandarian (2003). “Research advances in intelligent collision avoidance and adaptive cruise control”. In: *IEEE Transactions on Intelligent Transportation Systems* 4.3, pp. 143–153. DOI: [10.1109/tits.2003.821292](https://doi.org/10.1109/tits.2003.821292).
- Venthuruthiyil, S. P. and M. Chunchu (2022). “Anticipated Collision Time (ACT): A two-dimensional surrogate safety indicator for trajectory-based proactive safety assessment”. In: *Transportation Research Part C: Emerging Technologies* 139, p. 103655. DOI: [10.1016/j.trc.2022.103655](https://doi.org/10.1016/j.trc.2022.103655).
- Vogel, K. (May 2003). “A comparison of headway and time to collision as safety indicators”. In: *Accident Analysis & Prevention* 35.3, pp. 427–433. DOI: [10.1016/s0001-4575\(02\)00022-2](https://doi.org/10.1016/s0001-4575(02)00022-2).
- Wang, C., Y. Xie, H. Huang, and P. Liu (2021). “A review of surrogate safety measures and their applications in connected and automated vehicles safety modeling”. In: *Accident Analysis & Prevention* 157, p. 106157. DOI: [10.1016/j.aap.2021.106157](https://doi.org/10.1016/j.aap.2021.106157).
- Wang, X., J. Alonso-Mora, and M. Wang (2022). “Probabilistic Risk Metric for Highway Driving Leveraging Multi-Modal Trajectory Predictions”. In: *IEEE Transactions on Intelligent Transportation Systems* 23.10, pp. 19399–19412. DOI: [10.1109/tits.2022.3164469](https://doi.org/10.1109/tits.2022.3164469).
- Wang, Y., Z. Li, P. Liu, C. Xu, and K. Chen (2024). “Surrogate safety measures for traffic oscillations based on empirical vehicle trajectories prior to crashes”. In: *Transportation Research Part C: Emerging Technologies* 161, p. 104543. DOI: [10.1016/j.trc.2024.104543](https://doi.org/10.1016/j.trc.2024.104543).
- Ward, J. R., G. Agamennoni, S. Worrall, A. Bender, and E. Nebot (2015). “Extending Time to Collision for probabilistic reasoning in general traffic scenarios”. In: *Transportation Research Part C: Emerging Technologies* 51, pp. 66–82. DOI: [10.1016/j.trc.2014.11.002](https://doi.org/10.1016/j.trc.2014.11.002).
- Wessels, M., S. Kröling, and D. Oberfeld (2022). “Audiovisual time-to-collision estimation for accelerating vehicles: The acoustic signature of electric vehicles impairs pedestrians’ judgments”. In: *Transportation research part F: traffic psychology and behaviour* 91, pp. 191–212. DOI: [10.1016/j.trf.2022.09.023](https://doi.org/10.1016/j.trf.2022.09.023).
- Westhofen, L., C. Neurohr, T. Koopmann, M. Butz, B. Schütt, F. Utesch, B. Neurohr, C. Gutenkunst, and E. Böde (2022). “Criticality Metrics for Automated Driving: A Review and Suitability Analysis of the State of the Art”. In: *Archives of Computational Methods in Engineering* 30.1, pp. 1–35. DOI: [10.1007/s11831-022-09788-7](https://doi.org/10.1007/s11831-022-09788-7).
- Wu, K.-F. and P. P. Jovanis (2012). “Crashes and crash-surrogate events: Exploratory modeling with naturalistic driving data”. In: *Accident Analysis & Prevention* 45, pp. 507–516. DOI: [10.1016/j.aap.2011.09.002](https://doi.org/10.1016/j.aap.2011.09.002).
- Zheng, L., K. Ismail, and X. Meng (2014a). “Freeway safety estimation using extreme value theory approaches: A comparative study”. In: *Accident Analysis & Prevention* 62, pp. 32–41. DOI: [10.1016/j.aap.2013.09.006](https://doi.org/10.1016/j.aap.2013.09.006).

- Zheng, L., K. Ismail, and X. Meng (2014b). “Traffic conflict techniques for road safety analysis: open questions and some insights”. In: *Canadian Journal of Civil Engineering* 41.7, pp. 633–641. DOI: [10.1139/cjce-2013-0558](https://doi.org/10.1139/cjce-2013-0558).
- Zheng, L., T. Sayed, and F. Mannering (2021). “Modeling traffic conflicts for use in road safety analysis: A review of analytic methods and future directions”. In: *Analytic Methods in Accident Research* 29, p. 100142. DOI: [10.1016/j.amar.2020.100142](https://doi.org/10.1016/j.amar.2020.100142).
- Zhou, H. and Z. Zhong (2020). “Evasive behavior-based method for threat assessment in different scenarios: A novel framework for intelligent vehicle”. In: *Accident Analysis & Prevention* 148, p. 105798. DOI: [10.1016/j.aap.2020.105798](https://doi.org/10.1016/j.aap.2020.105798).